**UV-Raman Fingerprint of Brønsted Sites in MFI Zeolites: A Useful Marker in Dealumination Detection**

# UV-Raman Fingerprint of Brønsted Sites in MFI Zeolites: a Useful Marker in Dealumination Detection

*Matteo Signorile*[†], *Francesca Bonino*[†], *Alessandro Damin*[†], *Silvia Bordiga*[†]

† Department of Chemistry, NIS and INSTM Reference Centre, Università di Torino, Via G. Quarello 15, I-10135 and Via P. Giuria 7, I-10125, Torino, Italy

**Abstract**

In the present work a detailed UV-Raman characterization of a set of protonic MFI zeolites with variable Si/Al ratio is presented. A new vibrational feature was detected: interestingly such peak is present only when samples are carefully activated. Moreover its intensity is quantitatively related to the Al content of the framework through a direct law. On these basis, the origin of the vibrational mode can be attributed to the Brønsted acid site. The assignment was further supported by means of exchange experiments (with deuterium, sodium and ammonium), demonstrating the relevant contribution of the Brønsted proton in this peculiar vibration. Finally, by applying a steaming-like treatment (known to be able to induce dealumination), the observed decrease in the mode intensity was related to the leaching of Al atoms out of the framework, i.e. to the destruction of a fraction of the former Brønsted sites population. In this regard, the

monitoring by UV-Raman of such signal could represent an useful marker in detecting steaming and/or reaction induced dealumination in acidic zeolites.

## 1. Introduction

Acidic zeolites are relevant materials in the field of acid catalysis: thanks to their thermal stability and strong acidic behavior are largely exploited in refinery and petrolchemical process, such as the evergreen FCC (Fluid Catalytic Cracking) or the increasingly important MTH (Methanol To Hydrocarbons).[1-5] A serious drawback occurring at reaction condition is the progressive leaching of Al atoms from the framework with a concomitant lost of the associated Brønsted acidity. This process, commonly known as dealumination, can be considered as the main cause of the irreversible deactivation of acidic zeolite catalysts.[6-11]

Vibrational spectroscopy has been often applied in the characterization of acid zeolites: infrared spectroscopy allows to give a clear picture on the nature of the Brønsted acid sites and their interaction with probes and reactants, while Raman spectroscopy is useful in measuring the framework (i.e. collective) vibrational modes. [12-17] Nowadays most of the vibrational fingerprints of zeolites have been univocally interpreted, allowing to study the zeolites structure, reactivity as well as their dealumination.[16-19] With respect to the infrared one, the Raman characterization of zeolites usually involved much simpler approaches and experimental setups: apart from some pioneering studies,[20-23] most of the experiments were carried out in air, i.e. without considering the effect of hydration of the samples and their interaction with environmental molecules. The main reason is the difficulty to obtain good quality Raman spectra as a consequence of the photoemission of the samples, most probably ascribable to fluorescent, coke-like molecules adsorbed on the zeolite. The photoemission signal could be in most of the situations orders of

magnitudes more intense than the Raman one, making the last undetectable. The possible solutions to such problems are: i) to perform oxidative activation treatments (e.g. pure oxygen flow at high temperature) and to avoid the sample re-exposure to the environment; ii) to exploit an excitation laser far from the typical emission range of coke-like species, e.g. in the UV spectral region.[24]

In the present study these two methodologies have been efficiently combined in order to obtain high quality Raman spectra on a selected pool of acidic zeolites with MFI structure: a new vibrational feature related to the Brønsted acid site was reported for the first time. The new Raman fingerprint can be exploited in revealing dealumination, in a more sensitive way with respect to FTIR.

## 2. Experimental

A homogeneous set of MFI zeolites, with comparable surface area, was selected: the samples, supplied by Zeolyst in their ammonic form, are characterized by increasing Si/Al ratios in the range 140 – 12 as reported in Table 1. Samples will be labeled in the following as *X*-MFI-*yy*, where *X* represents the chemical form of the zeolite (H for protonic, $NH_4$ for ammonic, Na for sodic) and *yy* is the Si/Al ratio.

| Sample label | Commercial name | Si/Al[a] | Surface area[a] $m^2/g$ |
|---|---|---|---|
| MFI-12 | CBV 2314 | 11.5 | 425 |
| MFI-15 | CBV 3014E | 15 | 405 |
| MFI-25 | CBV 5524G | 25 | 425 |
| MFI-40 | CBV 8014 | 40 | 425 |
| MFI-140 | CBV 28014 | 140 | 400 |

a. Data from producer.

**Table 1.** List of the samples presented in this work.

All the zeolites were first converted in their protonic form by static air calcinations (5 hours at 550 °C, 5 °C/min ramp) and consequently activated (i.e. dehydrated and cleaned from organic residuals) before to characterize them. The treatment was performed in the same cell where the measurement was later on carried out, so avoiding its re-exposure to the external environment. The larger fraction of adsorbed water was removed by outgassing the samples for 1 hour under dynamic vacuum, starting from RT and progressively increasing the temperature to 150°C with a ramp of 5 °C/min. Then the combustion of organic residuals was performed by heating the sample under 100 mbar of pure oxygen from 150°C up to 550°C with a ramp of 5 °C/min and further leaving the sample under oxidizing atmosphere for 1 hour. Finally the sample was outgassed under dynamic vacuum at 550°C for 30 min in order to remove all the combustion residuals. The Na material was prepared by solution ion exchange according to the literature.[25] The deuterium exchange was performed in gas phase: the activated material was contacted with $D_2O$ vapors at RT (p = 25 mbar) for 30' and then outgassed at the same temperature to remove most of the physisorbed fraction. The procedure was repeated 3 times, then the sample was reactivated with the standard procedure in order to obtain a fully dehydrated material.

Dealumination was induced by fast heating the sample at 350 °C in contact with ~30 mbar (vapor pressure of water at 25°C): after 30' of reaction, the excess water was outgassed and complete dehydration was achieved by further raising the temperature up to 550°C with a rate of 5 °C/min and keeping it for more 30'. The procedure was later repeated on the same sample increasing the reaction temperature to 450 °C.

The UV-Raman spectra were collected by means of a Renishaw inVia Raman Microscope spectrometer, equipped with a 3600 lines/mm grating to disperse the scattered light on a UV enhanced, Peltier cooled CCD detector. The excitation beam was focused on the sample through a 15x objective. The Rayleigh peak was removed by a dielectric edge filter. A Coherent MotoFred 300C frequency doubled $Ar^+$ laser, emitting at 244 nm, was used as excitation source. The zeolite sample in pure form was measured as self-supported pellet under continuous rotation in order to exploit the full power of the laser at the samples (about 5 mW) avoiding beam induced damaging. The continuous rotation, exposing time by time a different spot on the surface of the pellet to the laser beam, avoids the overexposure of the sample possibly leading to its degradation. Almost 20 repeated spectra were collected for each sample, verifying that no variation (i.e. decomposition) is occurring along the measurements. In order to guarantee a proper comparison of the spectra in terms of intensities, these have been normalized: the symmetric Si-O-Si stretchings band centered at 800 $cm^{-1}$ was adopted as internal reference, as it shows negligible variations upon the different samples/treatments. This procedure further allows to prevent the effects related to the unstable focus on the sample, particularly severe in the case of the rotating setup adopted. FTIR analysis has been performed on a Bruker Vertex 70 FTIR, equipped with a HgCdTe cryogenic detector. Spectra were collected at a resolution of 2 $cm^{-1}$, averaging 32 scans. The sample has been prepared as thin self-supported pellet and measured in

an home-made cell. X-Ray Powder Diffraction patterns have been collected with a PW3050/60 X'Pert PRO MPD diffractometer from Panalytical working in Bragg–Brentano geometry, using as source the high power ceramic tube PW3373/10 LFF with a Cu anode (λ=1.541 Å), equipped with a Ni filter to attenuate the kβ line and an RTMS (Real Time Multiple Strip) X'celerator as detector. The same pellet used in the FTIR delaumination experiments was measured after re-exposing them to air. Patterns were collected in the $5° \leq 2\theta \leq 60°$ range with a 0.02° step.

## 3. Results and Discussion

The UV-Raman spectra of all MFI samples listed in Table 1 are reported in Figure 1: all the spectra show almost identical vibrational features in the low frequencies range, well described in the literature and ascribed to the vibrational modes of the different ring structures constituting the MFI framework. The most intense and sharp peak at about 380 $cm^{-1}$ is assigned to the 5-members rings typical of this structure, while the wide shoulder extending at higher frequencies has been attributed to the vibrational modes involving the other ring structures (10-, 6- and 4-member rings).[12-14] Concerning the Si-O-Si stretching regions, the signals ascribed to the asymmetric modes (around 1200 $cm^{-1}$) are quite similar as well, while some deviations are observed in the neighborhood of the band of the symmetric Si-O-Si stretchings (800 $cm^{-1}$). In detail, a clearly distinguishable peak is recognized around 745 $cm^{-1}$; furthermore, its intensity increases linearly as the Al content of the samples increases under the adopted experimental and treatment conditions (see Figure 1c).

The quantitative intensity dependence of the 745 $cm^{-1}$ band according to the Al framework concentration ratio suggests that such vibration is related to the Brønsted moiety. While no previous Raman results were reported in this regard, the INS characterization performed by Jobic and coworkers showed the presence of a multicomponent feature in the same spectral region

(maximum at 785 $cm^{-1}$):[26] thanks to the superior cross section of neutrons toward hydrogen, this feature is surely related to a vibration strongly involving the Brønsted proton. However the discussion on the physical origin of this band is limited, being attributed by the authors "to framework modes coupled with proton motions".

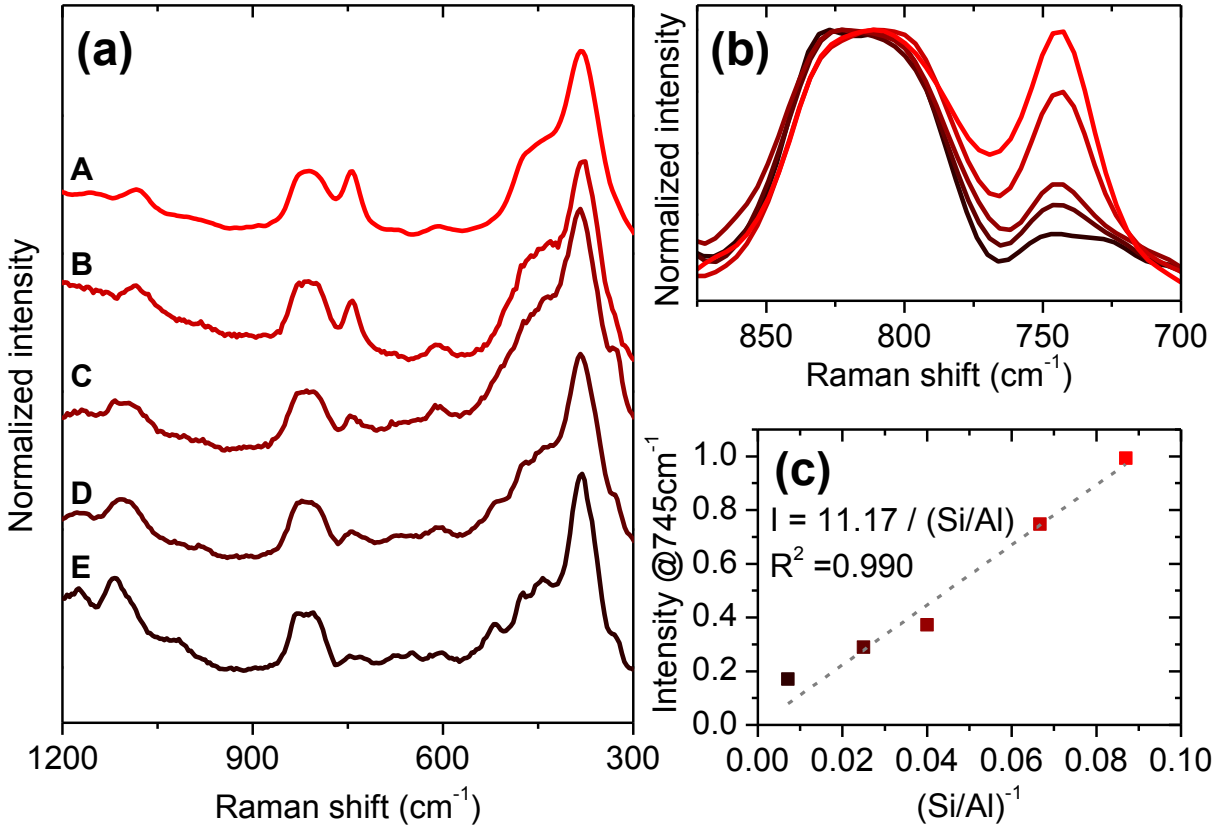


**Figure 1.** In part (a), the UV-Raman spectra of: **A** H-MFI-12; **B** H-MFI-15; **C** H-MFI-25; **D** H-MFI-40; and **E** H-MFI-140 samples in their activated form are reported. All the spectra have been normalized to the intensity of the 800 $cm^{-1}$ band and vertically translated for a better visualization. In part (b) a detail of the 745 $cm^{-1}$ band is given. Part (c) shows the intensities of the 745 $cm^{-1}$ band vs. the reciprocal of Si/Al ratio of all the H-MFI samples.

In order to get a deeper understanding on the origin of the 745 $cm^{-1}$ Raman peak, the higher Al content sample (H-MFI-12, showing the more intense and defined band) was further characterized. Three different approaches were adopted: i) deuterium exchange of the Brønsted site; ii) sodium ion exchange; and iii) dosage of a strong basic molecule (i.e. $NH_3$) able to react with protons of the Brønsted site. The UV-Raman spectra of these exchanged zeolites are reported in Figure 2.

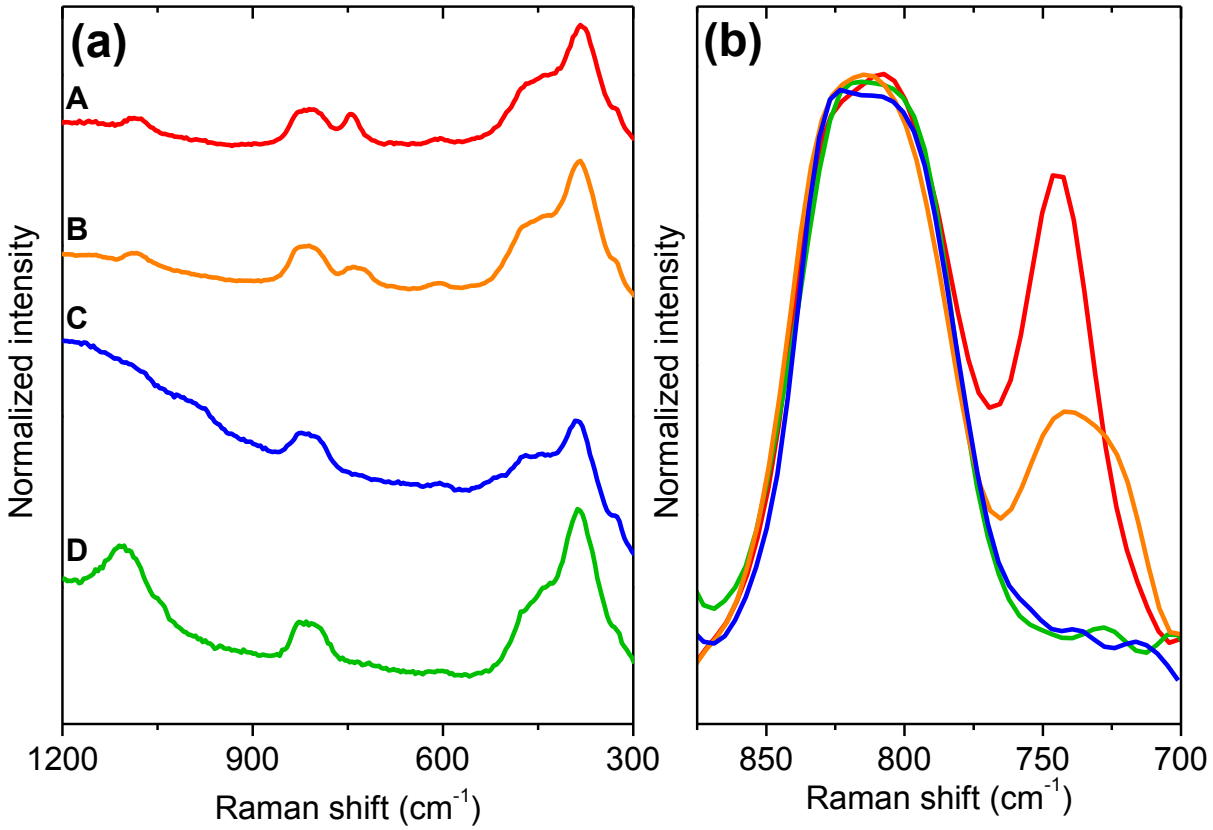


**Figure 2.** In part (a), the UV-Raman spectra of **A** H-MFI-12; **B** deuterium exchanged H-MFI-12; **C** Na-MFI-12; and **D** H-MFI-12 contacted with 50 mbar of gaseous $NH_3$ are shown. All the spectra have been normalized to the intensity of the 800 $cm^{-1}$ band and vertically translated for a better visualization. In part (b) a detail of the 745 $cm^{-1}$ band is given.

All the adopted strategies suggest that the vibrational mode is related to the proton of the Brønsted acid site. The deuterium exchange, even if only partial (see Figure S1 of the additional content for the FTIR detail on the OH and OD stretching regions), gave rise to a reduction of the intensity of the 745 $cm^{-1}$ mode, along with an enlargement of its bandwidth. Looking carefully at the peak shape, the presence of a second band red-shifted of approximately 20 $cm^{-1}$ can be inferred: the increase in the reduced mass of the vibrational mode due to the deuterium substitution suggests the relation among the signal and the proton of the Brønsted site. A further confirmation comes out from the spectrum of the Na-MFI-12 sample: in this case the Brønsted site is no longer observed because of the substitution of the proton with the heavier $Na^+$ cation, resulting in a complete erosion of the 745 $cm^{-1}$ peak. This result is in perfect agreement with FTIR (Figure S1): the 3610 $cm^{-1}$ band, associated to the Brønsted O-H stretching, follows the same trend reported for the 745 $cm^{-1}$ mode demonstrating the complete substitution of the proton by $Na^+$ cations. Also ammonia adsorption supports the previous observations: thanks to its basicity, $NH_3$ is able to react with the Brønsted proton with a simple acid-base reaction, i.e. by forming ammonium ions as reported in Figure S2: the growth of a band at 1450 $cm^{-1}$ demonstrated the occurrence of the reaction.[27] As already observed in the Na-MFI-12, also in the $NH_4$-MFI-12 spectrum the 745 $cm^{-1}$ band is no longer observed, as a consequence of the transformation of the protons in ammonium ions.

To finally check the previous claims, the reversibility of the ammonia adsorption was verified: a $NH_3$-TPD like experiment was performed by outgassing the $NH_4$-MFI-12 sample at increasing temperatures. The results are shown in Figure 3. As already depicted by Figure 2 curve D, the spectrum of the $NH_4$-MFI-12 (while in contact with 50 mbar of gaseous $NH_3$) doesn't show anymore the 745 $cm^{-1}$ peak as all the protons are converted in ammonium ions. Starting to outgas

the sample at RT no variations are observed concerning the 745 $cm^{-1}$ band, while the Raman spectrum is modified around 1100 $cm^{-1}$: the erosion of the large and intense mode observed in presence of gaseous ammonia can be associated to the desorption of the physisorbed, liquid-like $NH_3$ condensed in the zeolite pores.[28] As the temperature is increased the 745 $cm^{-1}$ signal is progressively recovered: already at 150 °C the peak, even if only partially, is clearly recovered. Consistently with $NH_3$-TPD literature data,[29-31] a relevant fraction of ammonium starts to be reconverted to proton and ammonia at around 250 °C, resulting in a further increase of the intensity of the related mode. Finally, reaching again 550 °C, all the Brønsted sites are recovered. It is interesting to underline that the intensity of the 745 $cm^{-1}$ band is increased with respect to the bare activation (shown in Figure 1). Possibly the absence of a large number of free protons up to quite high temperatures helps the activation by limiting the side reactivity of hydrocarbons toward coke-like species (hardly removable even by calcinations), meanwhile favoring their desorption and elimination. In this regard, the quantitative relation between the Si/Al ratio and the 745 $cm^{-1}$ band has to be carefully considered, since the activation step can lead to different outcomes (e.g. to a change of the slope of the calibration line reported in Figure 1c) depending on its real effectiveness. Furthermore the shape of the background, due to fluorescence interference, can drive to misleading reading of the intensities, even after the normalization procedure.

On the basis of the previous evidences, some hypothesis on the origin of the 745 $cm^{-1}$ band can be inferred. First of all, the vibration is expressed only in presence of the free Brønsted site proton, as the $Na^+$ substitution and the reaction with ammonia demonstrated univocally. Instead it is less trivial to define the type of atomic motion involving the proton and its neighbor atoms. On this regard, some suggestions arise from the partial deuteration experiment and in particular

from the estimated peak shift (-20 $cm^{-1}$). Considering as a rough model the vibrational modes of isolated surface silanols on fumed silica, upon deuterium exchange, the Si-OH stretching mode experimentally shows a similar shift (-13 $cm^{-1}$), while a Si-O-H bending is subjected to an approximately ten times bigger displacement.[32] Such difference is ascribable to the different weight of the proton in the normal coordinate associated to these vibrations, much larger in the bending case. This observation suggests that the 745 $cm^{-1}$ could be ascribed to Si-O-Al bridge stretching mode (also considering its energy, close to the one of Si-O-Si symmetric stretching modes). The motion of the proton is probably consequent to the displacement of the oxygen, with a low contribution to the normal coordinate of the overall vibration in agreement with the isotopic substitution experiment. Nevertheless, in order to get deeper insight in the mode assignment, quantum mechanical simulation represents the election necessary tool and further studies are required.

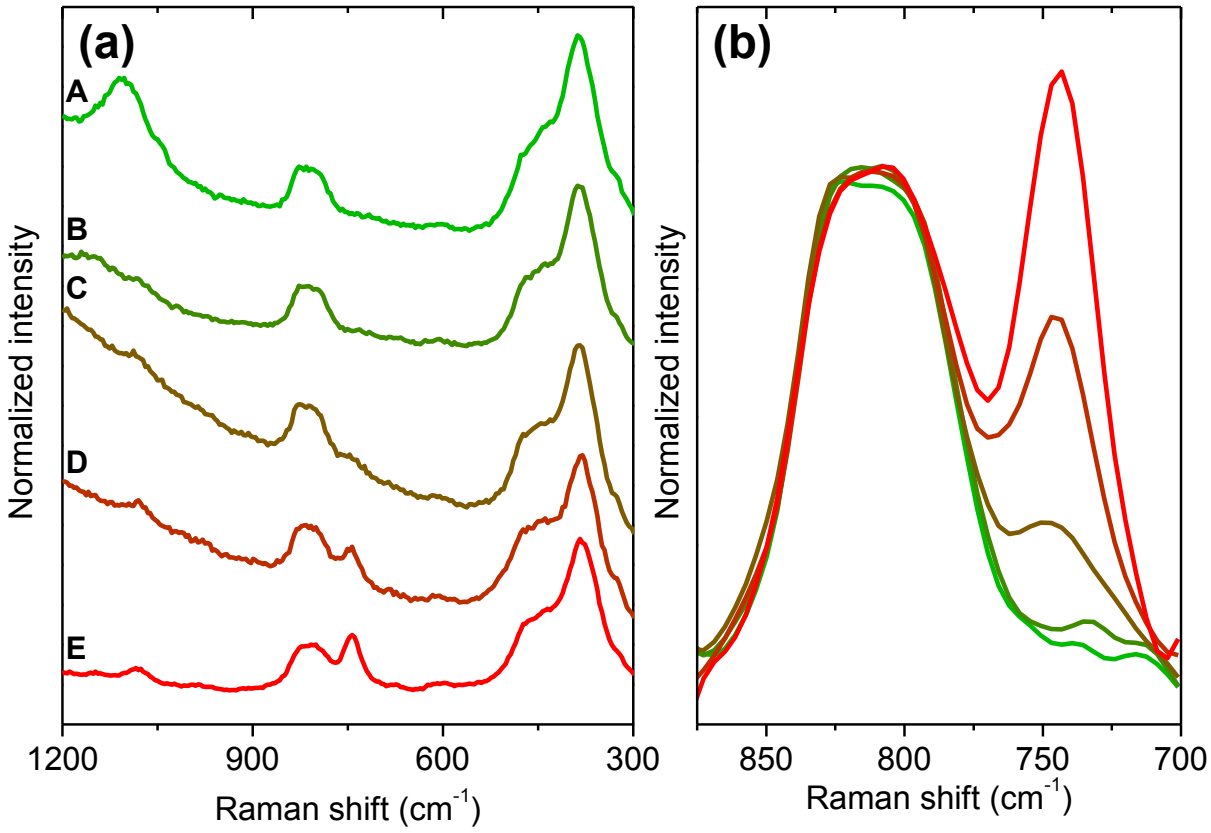


**Figure 3.** In part (a), the UV-Raman spectra of: **A** H-MFI-12 converted in $NH_4$-MFI-12 by dosing 50 mbar of $NH_3$ and then outgassed for 30' at **B** RT; **C** 150 °C; **D** 250 °C; and **E** 550 °C are shown. All the spectra have been normalized to the intensity of the 800 $cm^{-1}$ band and vertically translated for a better visualization. In part (b) a detail of the 745 $cm^{-1}$ band is given.

Since an univocal quantitative relation exists between the 745 $cm^{-1}$ mode and the Brønsted moiety, such signal can be exploited as a marker following the dealumination process, where the acid sites are progressively depleted by the leaching of the $Al^{3+}$ cations out of their framework positions. This process however does not imply long range structural effects, as the XRPD data reported in Figure S3 show: even after steaming, the patterns are completely unaltered. Under a vibrational point of view, dealumination can be detected looking at the OH stretching region in FTIR spectra, where some bands ascribed to Al-OH vibrational modes (3663 $cm^{-1}$ and 3780 $cm^{-}$

[1]) have been detected in MFI zeolites after prolonged steaming.[19,33] In the present work, milder conditions were applied in comparison to a standard steaming procedure, achieving a considerably lower extent of dealumination: FTIR spectra reported in Figure S4 show very weak manifestations for the Al-OH sites, difficult to observe especially at the lower dealumination degree.

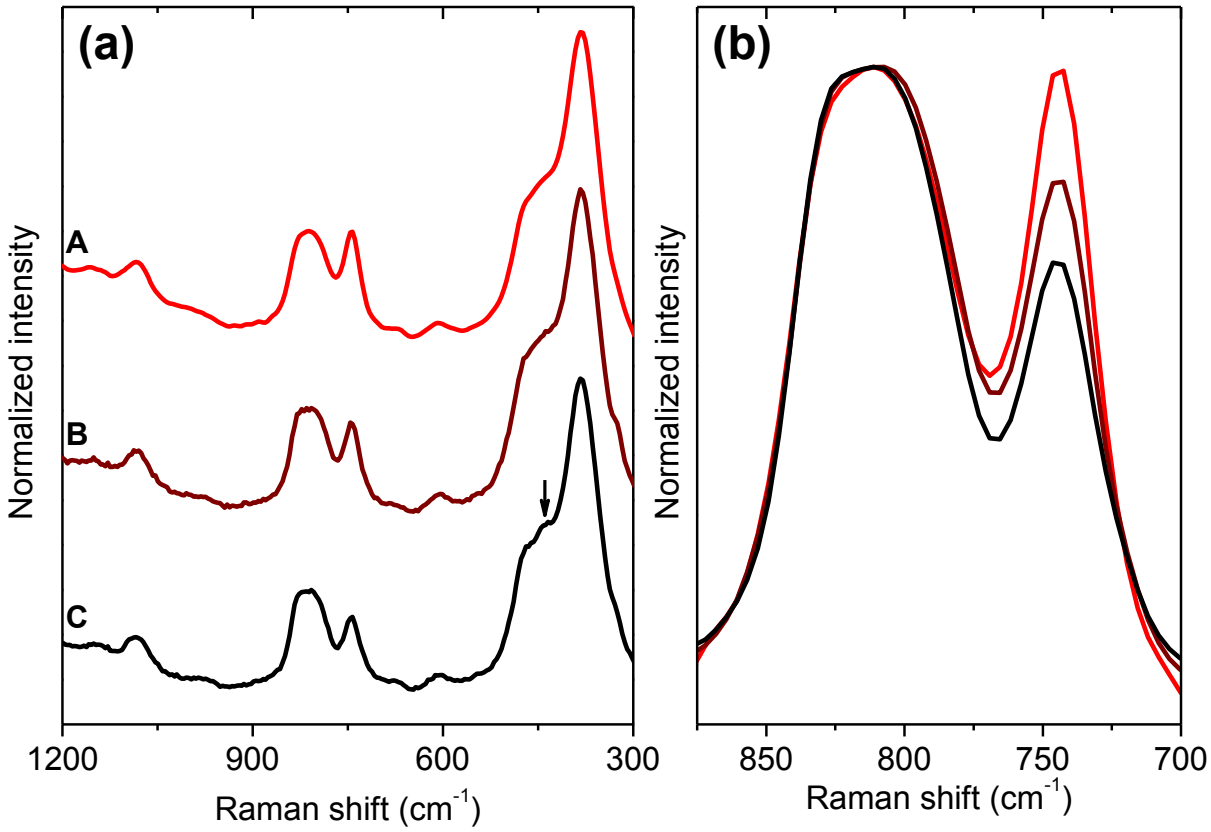


**Figure 4.** In part (a), the UV-Raman spectra of H-MFI-12 **A** activated; **B** after treatment under $H_2O$ vapor pressure at 350°C and reactivation; and **C** after treatment under $H_2O$ vapor pressure at 450°C and reactivation are shown. All the spectra have been normalized to the intensity of the 800 $cm^{-1}$ band and vertically translated for a better visualization. In part (b) a detail of the 745 $cm^{-1}$ band is given.

Conversely the UV-Raman spectra reported in Figure 4 delineate larger differences upon increasing dealumination: after the water treatment at 350 °C, the intensity of the 745 $cm^{-1}$ peak is reduced by approximately 20% with respect to the bare activated sample. Increasing the treatment temperature to 450°C, this reduction reaches about the 33%. By comparison, the intensity of the Brønsted site OH stretching measure by FTIR (3610 $cm^{-1}$) is unvaried along the treatments, while the 3663 $cm^{-1}$ band still shows a poor intensity even after treating at 450°C. Interestingly a further weak shoulder appears in the low frequency region (around 430 $cm^{-1}$, pointed out by the arrow in Figure 4) after the last dealumination step. A similar vibration is observed in the Raman spectrum of corundum,[34] possibly testifying the formation of octahedral extra framework Al species.

## 4. Conclusions

An unreported Raman active vibrational mode whose intensity is strictly related to the Al framework content in the MFI zeolites was identified. Its relation with the Brønsted acid site was demonstrated through several approaches. Even if the band shows a clear quantitative relation with the Al content of the framework a real quantification procedure is demanding because of side effects (e.g. quality and type of sample activation, fluorescence), making complex a correct estimation of the peak intensity. However, thanks to the sensitivity to the Brønsted sites concentration, the 745 $cm^{-1}$ mode can be regarded as an interesting marker for processes causing a modification in the Brønsted sites population, e.g. dealumination caused by steaming processes.

## Supporting Information

The Supporting Information is available free of charge on the ACS Publications website.

FTIR spectra of the Na-MFI-12 and H-MFI-12 before and after deuterium exchange, FTIR spectra of activated H-MFI-12 and it conversion in $NH_4$-MFI-12, XRPD patterns and FTIR spectra of the H-MFI-12 sample before and after dealumination treatment.


## Acknowledgment

The authors acknowledge prof. Karl Petter Lillerud (University of Oslo), prof. Stian Svelle (University of Oslo) and dr. Pablo Beato (Haldor Topsøe A/S) for providing the samples and Open Access Labs project for funding (2013-2015 agreement of Compagnia di San Paolo and Università di Torino).


## References


1. Bjorgen, M.; Svelle, S.; Joensen, F.; Nerlov, J.; Kolboe, S.; Bonino, F.; Palumbo, L.; Bordiga, S.; Olsbye, U. Conversion of Methanol to Hydrocarbons over Zeolite H-Zsm-5: On the Origin of the Olefinic Species. *J. Catal.* **2007**, *249*, 195-207.

2. Martinez, C.; Corma, A. Inorganic Molecular Sieves: Preparation, Modification and Industrial Application in Catalytic Processes. *Coord. Chem. Rev.* **2011**, *255*, 1558-1580.

3. Teketel, S.; Skistad, W.; Benard, S.; Olsbye, U.; Lillerud, K. P.; Beato, P.; Svelle, S. Shape Selectivity in the Conversion of Methanol to Hydrocarbons: The Catalytic Performance of One-Dimensional 10-Ring Zeolites: Zsm-22, Zsm-23, Zsm-48, and Eu-1. *ACS Catal.* **2012**, *2*, 26-37.

4. Olsbye, U.; Svelle, S.; Bjorgen, M.; Beato, P.; Janssens, T. V. W.; Joensen, F.; Bordiga, S.; Lillerud, K. P. Conversion of Methanol to Hydrocarbons: How Zeolite Cavity and Pore Size Controls Product Selectivity. *Angew. Chem.-Int. Edit.* **2012**, *51*, 5810-5831.

5. Vogt, E. T. C.; Weckhuysen, B. M. Fluid Catalytic Cracking: Recent Developments on the Grand Old Lady of Zeolite Catalysis. *Chem. Soc. Rev.* **2015**, *44*, 7342-7370.

6. Gayubo, A. G.; Aguayo, A. T.; Olazar, M.; Vivanco, R.; Bilbao, J. Kinetics of the Irreversible Deactivation of the Hzsm-5 Catalyst in the Mto Process. *Chem. Eng. Sci.* **2003**, *58*, 5239-5249.

7. Gayubo, A. G.; Aguayo, A. T.; Atutxa, A.; Prieto, R.; Bilbao, J. Deactivation of a Hzsm-5 Zeolite Catalyst in the Transformation of the Aqueous Fraction of Biomass Pyrolysis Oil into Hydrocarbons. *Energy Fuels* **2004**, *18*, 1640-1647.

8. Gayubo, A. G.; Aguayo, A. T.; Atutxa, A.; Prieto, R.; Bilbao, J. Role of Reaction-Medium Water on the Acidity Deterioration of a Hzsm-5 Zeolite. *Ind. Eng. Chem. Res.* **2004**, *43*, 5042-5048.

9. Cerqueira, H. S.; Caeiro, G.; Costa, L.; Ribeiro, F. R. Deactivation of Fcc Catalysts. *J. Mol. Catal. A: Chem.* **2008**, *292*, 1-13.

10. Corma, A.; Mengual, J.; Miguel, P. J. Stabilization of Zsm-5 Zeolite Catalysts for Steam Catalytic Cracking of Naphtha for Production of Propene and Ethene. *Appl. Catal., A* **2012**, *421*, 121-134.

11. Ibanez, M.; Gamero, M.; Ruiz-Martinez, J.; Weckhuysen, B. M.; Aguayo, A. T.; Bilbao, J.; Castano, P. Simultaneous Coking and Dealumination of Zeolite H-Zsm-5 During the Transformation of Chloromethane into Olefins. *Catal. Sci. Technol.* **2016**, *6*, 296-306.

12. Dutta, P. K.; Rao, K. M.; Park, J. Y. Correlation of Raman Spectra of Zeolites with Framework Architecture. *J. Phys. Chem.* **1991**, *95*, 6654-6656.

13. Knops-Gerrits, P.-P.; De Vos, D. E.; Feijen, E. J. P.; Jacobs, P. A. Raman Spectroscopy on Zeolites. *Microporous Mater.* **1997**, *8*, 3-17.

14. Scarano, D.; Zecchina, A.; Bordiga, S.; Geobaldo, F.; Spoto, G.; Petrini, G.; Leofanti, G.; Padovan, M.; Tozzola, G. Fourier-Transform Infrared and Raman-Spectra of Pure and Al-Substituted, B-Substituted, Ti-Substituted and Fe-Substituted Silicalites - Stretching-Mode Region. *J. Chem. Soc. Faraday Trans.* **1993**, *89*, 4123-4130.

15. Zecchina, A.; Spoto, G.; Bordiga, S. Probing the Acid Sites in Confined Spaces of Microporous Materials by Vibrational Spectroscopy. *Phys. Chem. Chem. Phys.* **2005**, *7*, 1627-1642.

16. Holm, M. S.; Svelle, S.; Joensen, F.; Beato, P.; Christensen, C. H.; Bordiga, S.; Bjorgen, M. Assessing the Acid Properties of Desilicated Zsm-5 by Ftir Using Co and 2,4,6-Trimethylpyridine (Collidine) as Molecular Probes. *Appl. Catal. A-Gen.* **2009**, *356*, 23-30.

17. Bordiga, S.; Lamberti, C.; Bonino, F.; Travert, A.; Thibault-Starzyk, F. Probing Zeolites by Vibrational Spectroscopies. *Chem. Soc. Rev.* **2015**, *44*, 7262-7341.

18. Campbell, S. M.; Bibby, D. M.; Coddington, J. M.; Howe, R. F.; Meinhold, R. H. Dealumination of Hzsm-5 Zeolites .1. Calcination and Hydrothermal Treatment. *J. Catal.* **1996**, *161*, 338-349.

19. Szanyi, J.; Paffett, M. T. The Adsorption of Carbon Monoxide on H-Zsm-5 and Hydrothermally Treated H-Zsm-5. *Microporous Mater.* **1996**, *7*, 201-218.

20. Bremard, C.; Le Maire, M. Low-Frequency Raman Spectra of Dehydrated Faujasitic Zeolites. *J. Phys. Chem.* **1993**, *97*, 9695-9702.

21. Li, C.; Stair, P. C. Ultraviolet Raman Spectroscopy Characterization of Coke Formation in Zeolites. *Catal. Today* **1997**, *33*, 353-360.

22. Chua, Y. T.; Stair, P. C. An Ultraviolet Raman Spectroscopic Study of Coke Formation in Methanol to Hydrocarbons Conversion over Zeolite H-Mfi. *J. Catal.* **2003**, *213*, 39-46.

23. Beato, P.; Schachtl, E.; Barbera, K.; Bonino, F.; Bordiga, S. Operando Raman Spectroscopy Applying Novel Fluidized Bed Micro-Reactor Technology. *Catal. Today* **2013**, *205*, 128-133.

24. Fan, F.; Feng, Z.; Li, C. Uv Raman Spectroscopic Studies on Active Sites and Synthesis Mechanisms of Transition Metal-Containing Microporous and Mesoporous Materials. *Accounts Chem. Res.* **2010**, *43*, 378-387.

25. Silva, B.; Figueiredo, H.; Soares, O. S. G. P.; Pereira, M. F. R.; Figueiredo, J. L.; Lewandowska, A. E.; Banares, M. A.; Neves, I. C.; Tavares, T. Evaluation of Ion Exchange-Modified Y and Zsm5 Zeolites in Cr(Vi) Biosorption and Catalytic Oxidation of Ethyl Acetate. *Appl Catal B.* **2012**, *117*, 406-413.

26. Jobic, H.; Tuel, A.; Krossner, M.; Sauer, J. Water in Interaction with Acid Sites in H-Zsm-5 Zeolite Does Not Form Hydroxonium Ions. A Comparison between Neutron Scattering Results and Ab Initio Calculations. *J. Phys. Chem.* **1996**, *100*, 19545-19550.

27. Zecchina, A.; Marchese, L.; Bordiga, S.; Paze, C.; Gianotti, E. Vibrational Spectroscopy of Nh4+ Ions in Zeolitic Materials: An Ir Study. *J. Phys. Chem. B* **1997**, *101*, 10128-10135.

28. Ujike, T.; Tominaga, Y. Raman Spectral Analysis of Liquid Ammonia and Aqueous Solution of Ammonia. *J. Raman Spectrosc.* **2002**, *33*, 485-493.

29. Barthos, R.; Lónyi, F.; Onyestyák, G.; Valyon, J. Ir, Fr, and Tpd Study on the Acidity of H-Zsm-5, Sulfated Zirconia, and Sulfated Zirconia-Titania Using Ammonia as the Probe Molecule. *J Phys Chem B* **2000**, *104*, 7311-7319.

30. Lónyi, F.; Valyon, J. A Tpd and Ir Study of the Surface Species Formed from Ammonia on Zeolite H-Zsm-5, H-Mordenite and H-Beta. *Thermochim Acta* **2001**, *373*, 53-57.

31. Hunger, B.; Heuchel, M.; Clark, L. A.; Snurr, R. Q. Characterization of Acidic Oh Groups in Zeolites of Different Types: An Interpretation of Nh3-Tpd Results in the Light of Confinement Effects. *J Phys Chem B* **2002**, *106*, 3882-3889.

32. Boccuzzi, F.; Coluccia, S.; Ghiotti, G.; Morterra, C.; Zecchina, A. Infrared Study of Surface Modes on Silica. *J. Phys. Chem.* **1978**, *82*, 1298–1303.

33. Brand, H. V.; Redondo, A.; Hay, P. J. Theoretical Studies of Co Adsorption on H-Zsm-5 and Hydrothermally Treated H-Zsm-5. *J. Mol. Catal. A-Chem.* **1997**, *121*, 45-62.

34. Xu, J. A.; Huang, E.; Lin, J. F.; Xu, L. Y. Raman Study at High Pressure and the Thermodynamic Properties of Corundum: Application of Kieffer's Model. *Am. Miner.* **1995**, *80*, 1157-1165.

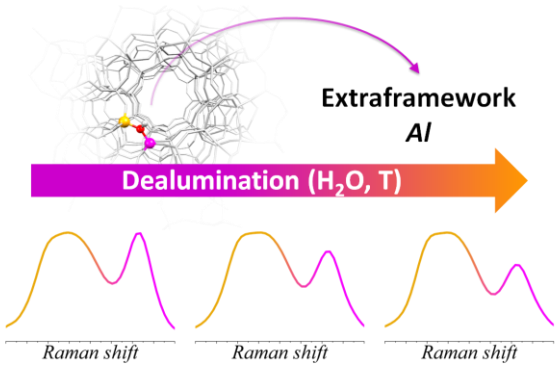
Extraframework
Al
Dealumination ($H_2O$, T)
Raman shift
Raman shift
Raman shift

# Supporting Information for:

# UV-Raman Fingerprint of Brønsted Sites in MFI Zeolites: a Useful Marker in Dealumination Detection

*Matteo Signorile[†], Francesca Bonino*[†], Alessandro Damin[†], Silvia Bordiga[†]*

† Department of Chemistry, NIS and INSTM Reference Centre, Università di Torino, Via G. Quarello 15, I-10135 and Via P. Giuria 7, I-10125, Torino, Italy

* Francesca Bonino, Tel: +39-011-6708383, Fax: +39-011-6707855, E-mail: francesca.bonino@unito.it

In order to verify the successfulness of the ion exchange procedures, FTIR spectra were collected. The spectra reported in the OH and OD stretching region Figure S1 demonstrated as only a partial deuterium exchange was achieved (approximately 50% of Brønsted sites were deuterated): the peak related to Brønsted sited red-shifts from 3610 $cm^{-1}$ to 2265 $cm^{-1}$ due to the increase in the reduced mass of the OH stretching mode upon deuterium exchange. Also the signal ascribed to isolated silanols OH stetchings shows the occurrence of a partial exchange, as testified by the reduction in intensity of the 3745 $cm^{-1}$ peak together with the appearance of a new signal at 2760 $cm^{-1}$. Instead, the sodium exchange was complete as the complete disappearing of the band of Brønsted sites OH stretchings demonstrates.

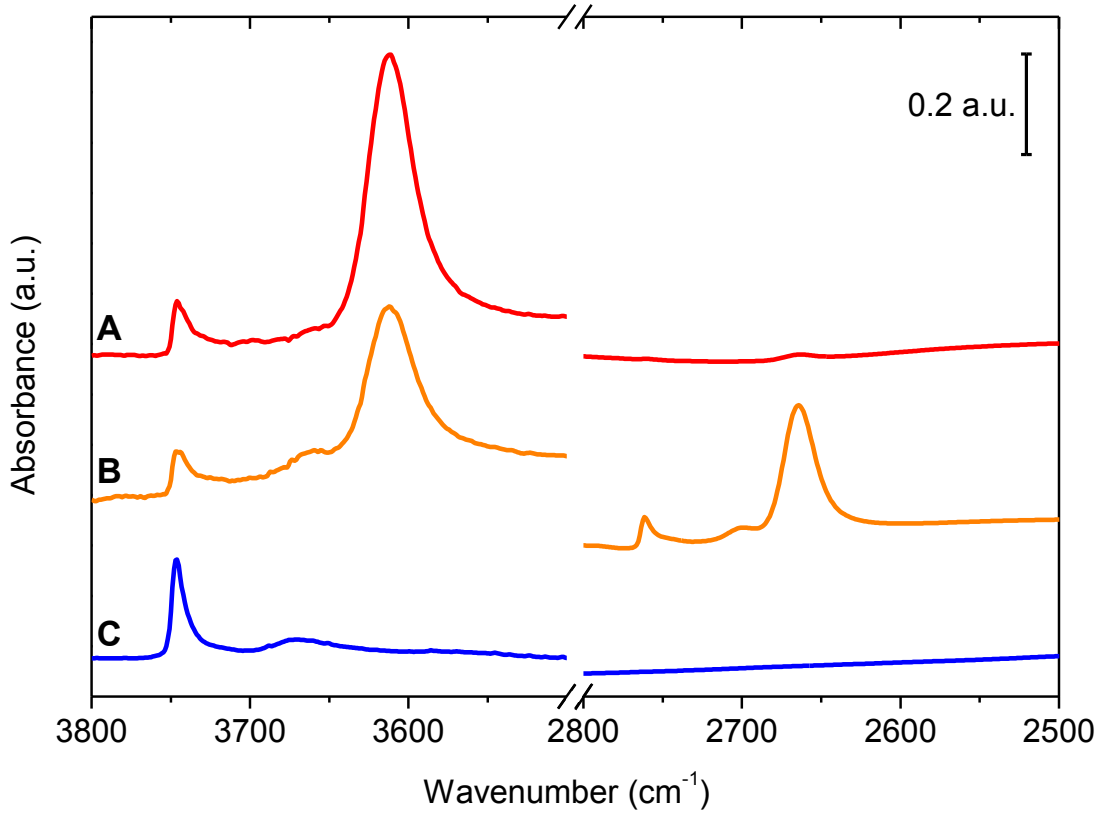


**Figure S1.** FTIR spectra of sample H-MFI-12 **A** activated as such; **B** activated after deuterium exchange; and **C** activated after Na exchange (i.e. Na-MFI-12).

In Figure S2 the FTIR spectrum of the H-MFI-12 sample is compared with the one obtained upon $NH_3$ contact. Furthermore, the $NH_4$-MFI-12 was outgassed for 30' to remove the physisorbed ammonia. The acid-base reaction occurring between the $NH_3$ and the Brønsted protons gives rise to the complete consumption of the latter, as testified by the disappearance of their O-H stretching band at 3610 $cm^{-1}$. Ammonium is then clearly formed according to the growth of an intense peak with maximum at 1450 $cm^{-1}$, univocally ascribable to the presence of the $NH_4^+$ moiety.[1] A further confirmation arises from the spectrum of $NH_4$-MFI-12 collected after 30' of outgassing: the ammonium signal is still present and the peak of ν(O-H) of Brønsted sites is not recovered. However the (partial) removal of physisorbed ammonia is observed as testified by the intensity decrease of the band at 1630 $cm^{-1}$, attributed to $NH_3$ bending.

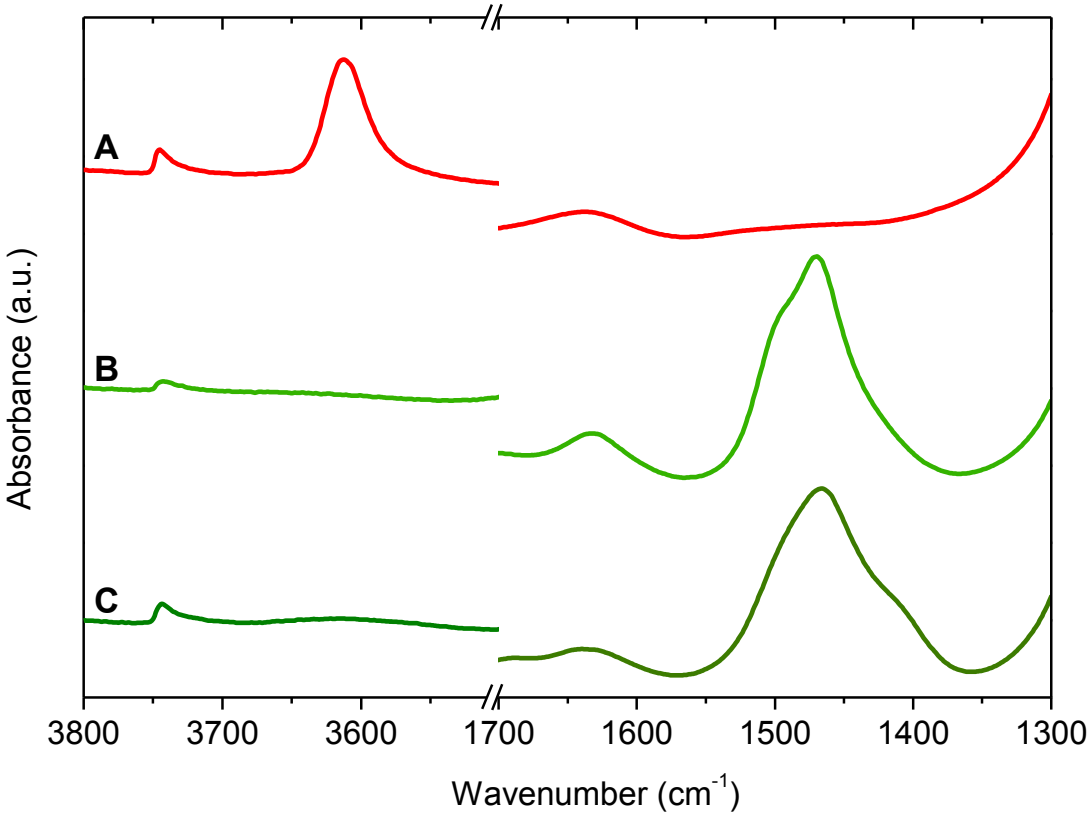


**Figure S2.** FTIR spectra of sample H-MFI-12 **A** activated as such; **B** converted in $NH_4$-MFI-12 by dosing 50 mbar of $NH_3$ and **C** outgassed for 30' to remove physisorbed ammonia.

Even if the Al is partially leached out from the framework because of the dealumination treatment, the overall crystal structure of the zeolite remains unaffected as the XRPD patterns reported in Figure S3 (where no difference are observed after the water treatment) demonstrate. The FTIR spectra of increasingly dealuminated samples are reported in Figure S4. According to literature, the two weak bands observed in the water treated samples at 3780 $cm^{-1}$ and 3663 $cm^{-1}$ are ascribed to Al-OH moieties formed upon hydrolysis of Al-O-Si bridges, i.e. testifying the dealumination of the zeolite.[2,3]

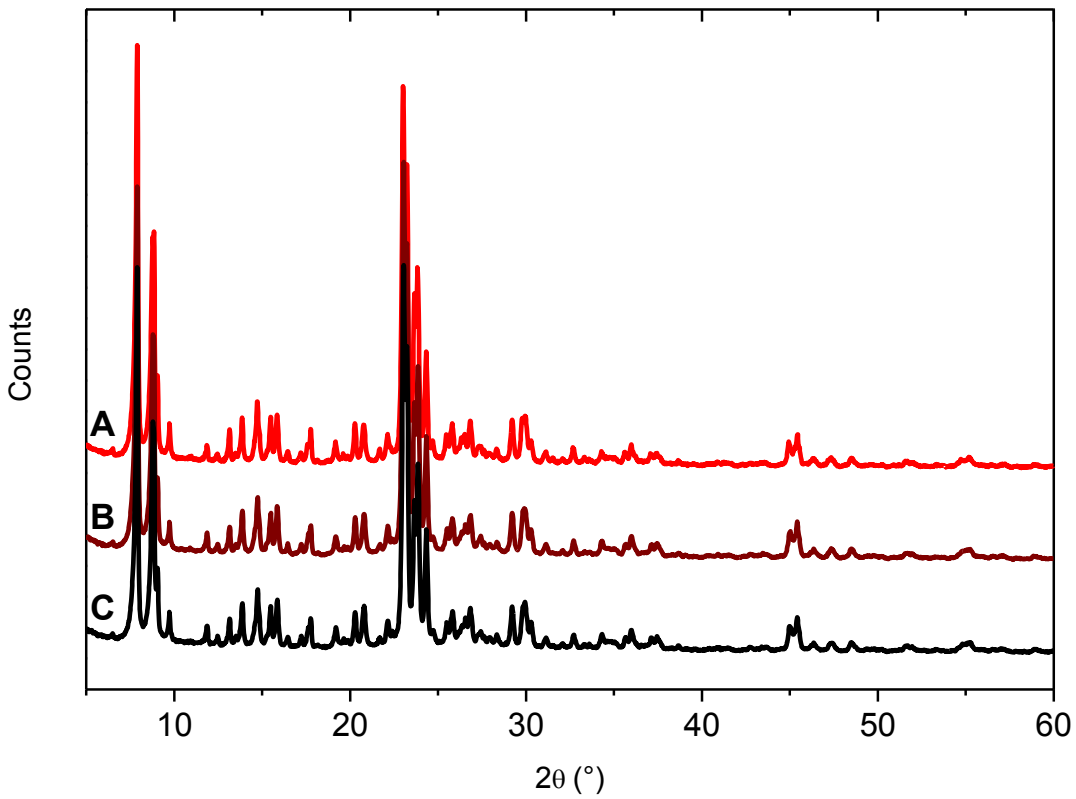


**Figure S3.** XRPD patterns of sample H-MFI-12 **A** activated; **B** after treatment under $H_2O$ vapor pressure at 350°C and reactivation; and **C** after treatment under $H_2O$ vapor pressure at 450°C and reactivation. The measure were collected in air. The patterns have been vertically translated for a better visualization.

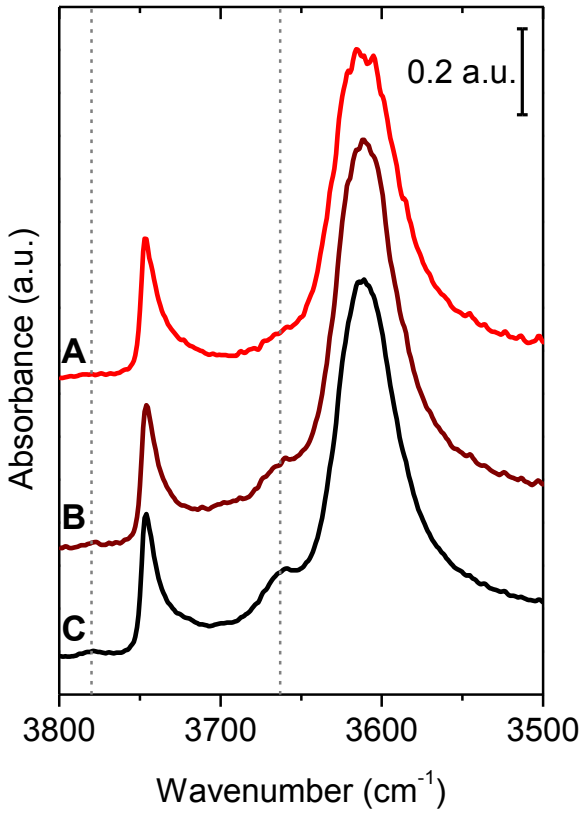


**Figure S4.** FTIR spectra of sample H-MFI-12 **A** activated; **B** after treatment under $H_2O$ vapor pressure at 350°C and reactivation; and **C** after treatment under $H_2O$ vapor pressure at 450°C and reactivation. The vertical dashed lines at 3780 $cm^{-1}$ and 3663 $cm^{-1}$ show the frequencies of typical dealumination fingerprints.

**References**

1. Zecchina, A.; Marchese, L.; Bordiga, S.; Paze, C.; Gianotti, E. Vibrational Spectroscopy of Nh4+ Ions in Zeolitic Materials: An Ir Study. *J. Phys. Chem. B* **1997**, *101*, 10128-10135.

2. Szanyi, J.; Paffett, M. T. The Adsorption of Carbon Monoxide on H-Zsm-5 and Hydrothermally Treated H-Zsm-5. *Microporous Mater.* **1996**, *7*, 201-218.

3. Brand, H. V.; Redondo, A.; Hay, P. J. Theoretical Studies of Co Adsorption on H-Zsm-5 and Hydrothermally Treated H-Zsm-5. *J. Mol. Catal. A-Chem.* **1997**, *121*, 45-62.